Maximizing the piezoelectric properties of thin film $Pb(Mg_{1/3}Nb_{2/3})O_3 - PbTiO_3$

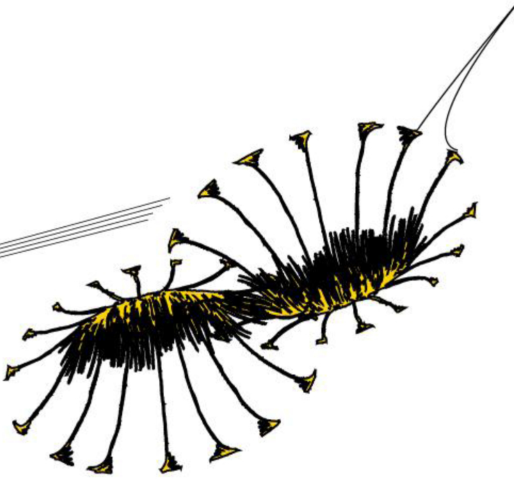

Jaap Geessinck & Maikel Gerritsen
Supervised by Matthijn Dekkers

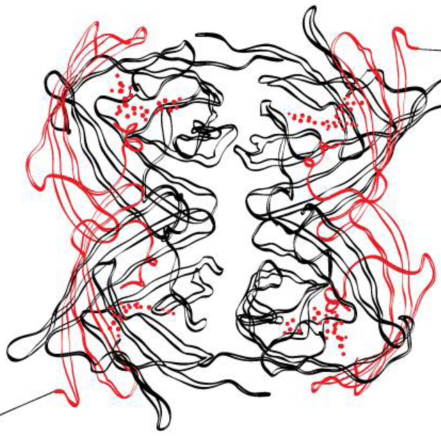

Bachelor Thesis
July 2012

Faculty of Science and Technology
Inorganic Materials Science Group

UNIVERSITY OF TWENTE.

Preface

After three years of education it is time to bring our obtained knowledge to the test. The Inorganic Material Science group had an interesting bachelor assignment in the field of piezoelectricity, which we were interested in. After a talk with our supervisor, Matthijn Dekkers, we were sure: our bachelor thesis had to be done at this group. The field of research we were working in already existed for quite a long time, but the material we were working with was very new within the group. The research was started in response to an article published on November 18th of 2011.

This material was new within the Inorganic Material Science group (IMS), so little was known on forehand. Because of this, the making of a sample with this material was the first time for our supervisor as well. What makes us feel like doing something new. This was really motivating for us.

The research done at the group was a completely different experience than any other course, project or experiment followed during our bachelor program. The biggest difference is the freedom which is given to you. The freedom to do the measurements the way we want to. To give an own twist to what we are doing, within the boundary conditions of the project. In the beginning this was a little uncomfortable, because we were searching for what we wanted to do. After the literature study we stated our goals and had an idea how we wanted to reach these. Now, after eleven weeks, we are satisfied with what we achieved. There are a lot of things we would have done different if we could do it again. But this is a good thing, while it means that we have learned a lot during this project.

The committee for this bachelor thesis consists of the following persons:

Prof. dr. ing. A.J.H.M. Rijnders - Chairman
Dr. Ir. J.M. Dekkers - Supervisor
Dr. J.W.J Verschuur - Exam committee

Abstract

Thin films of PMN-PT have been successfully grown on substrates of STO, as well as on silicon. For the deposition of PMN-PT on silicon, buffer layers of YSZ and CeO_2 were used. It is not yet achieved to grow a pure perovskite, epitaxial, (001)-orientated film of PMN-PT on a silicon substrate without a layer of STO. In the Si/YSZ/CeO_2/LNO/PMN-PT sample the pyrochloric (004)-orientation is still present. Next to that there are more perovskite orientations because the layer underneath, LNO, did not grow epitaxial. Nevertheless, the P-E loop looks good. Due to a lack of time the $e_{31,f}$ coefficient is not yet determined. The d_{33} coefficient of the STO/LNO/PMN-PT and the Si/STO/LNO/PMN-PT sample have been determined to be 135 and 100 pm/V respectively, which compared to PZT is not that high.

Contents

1 Introduction 1

2 Theory behind the piezoelectric effect 3
- 2.1 Piezoelectricity and polarization . . . 3
- 2.2 Influence on piezoelectricity . . . 5
- 2.3 PMN-PT . . . 7
- 2.4 Leakage current . . . 8
- 2.5 Introduction to Pulsed Laser Deposition (PLD) . . . 8
- 2.6 Direction of growth and lattice constant of crystals . . . 10
- 2.7 Miller Indices . . . 11
- 2.8 Producing a sample with PLD . . . 12
  - 2.8.1 STO → PMN-PT . . . 13
  - 2.8.2 Si → STO → PMN-PT . . . 14
  - 2.8.3 Si → STO → SRO → PMN-PT → SRO/Pt . . . 14
  - 2.8.4 Si → SRO → PMN-PT → Pt . . . 14
  - 2.8.5 Si → YSZ → CeO_2 → SRO/LNO → PMN-PT → Pt . . . 15

3 Characterisation Methods 16
- 3.1 X-Ray Diffraction (XRD) . . . 16
  - 3.1.1 2θ-scan . . . 17
  - 3.1.2 ϕ-scan . . . 17
- 3.2 Hysteresis loop . . . 17
- 3.3 Measuring the piezoelectric coefficient $e_{31,f}$ . . . 18
- 3.4 Measuring d_{33} . . . 19
- 3.5 Measuring d_{31} . . . 20

4 Results 23
- 4.1 STO/PMN-PT . . . 23
- 4.2 STO/LNO/PMN-PT . . . 26
- 4.3 Si/STO/LNO/PMN-PT . . . 28
- 4.4 Alternative method - Si/YSZ/CeO_2/LNO/PMN-PT . . . 31
- 4.5 PZT sample to determine $e_{31,f}$ . . . 33

5 Discussion & Conclusion 34
- 5.1 Discussion . . . 34
- 5.2 Conclusion . . . 35

6 Recommendations 37

7 Acknowledgements **38**

8 Planning **39**

9 Appendix **40**
9.1 STO/PMN-PT 40
9.2 STO/LNO/PMN-PT 41
9.3 Si/STO/LNO/PMN-PT 42
9.4 Si/YSZ/CeO_2/LNO/PMN-PT 43

List of abbreviations

E	Electric field
E_C	Coercive field
IMS	Inorganic Material Science group
LDV	Laser Doppler Vibrometer
LNO	Lanthanum Nickel Oxide
LSMO	Lanthanum Strontium Manganese Oxide
MBE	Molecular Beam Epitaxy
MEMS	Microelectromechanical system
MPB	Morphotropic phase Boundary
P	Polarization
P-E	Polarization against Electric field
P_R	Remanent polarization
PLD	Pulsed laser deposition
PMN-PT	$Pb(Mg_{1/3}Nb_{2/3})O_3 - PbTiO_3$
PZT	$Pb(Zr_xTi_{1-x})$
SEM	Scanning Electron Microscope
Si	Silicon
SRO	Strontium Ruthenate
STO	Strontium Titanate
T_C	Curie temperature
XRD	X-ray diffraction
YSZ	Yttria-stabilized zirconia

List of figures

Figure 2.1 page 4
Figure 2.2 page 5
Figure 2.3 page 6
Figure 2.4 page 6
Figure 2.5 page 7
Figure 2.6 page 9
Figure 2.7 page 12
Figure 2.8 page 13
Figure 2.9 page 15
Figure 3.1 page 18
Figure 3.2 page 20
Figure 4.1 page 25
Figure 4.2 page 25
Figure 4.3 page 27
Figure 4.4 page 27
Figure 4.5 page 28
Figure 4.6 page 29
Figure 4.7 page 30
Figure 4.8 page 30
Figure 4.9 page 31
Figure 4.10 page 32
Figure 4.11 page 33
Figure 8.1 page 41
Figure 8.2 page 42

List of tables

Table 4.1 page 24
Table 4.2 page 26
Table 4.3 page 31
Table 8.1 page 40
Table 8.2 page 40
Table 8.3 page 41
Table 8.4 page 42
Table 8.5 page 43

Chapter 1

Introduction

At the 18th of November in 2011 an article was published in Science, called: "Giant Piezoelectricity on Si for hyperactive MEMS" [1]. The scientists behind this paper have succeeded to achieve the growth of PMN-PT with an almost pure perovskite phase which possesses a giant piezoelectric response. This might just be a breakthrough for the broad implementation of active MEMS, where materials with these high piezoelectric properties are needed.

What will be done in this research is: trying to deposit a thin film layer of PMN-PT on a substrate, in which the PMN-PT got high piezoelectric properties. This is done with a technique called 'pulsed laser deposition' (PLD).

The first step will be to obtain a film of PMN-PT consisting of near pure perovskite phase. When this succeeds, conducting layers will have to placed on top and beneath the film to measure the electric properties of the material. Also the substrate has to be eventually made suitable for bending. This way the piezoelectric coefficients, like $e_{31,f}$ can be measured [2]. Measuring the coefficients such as $e_{31,f}$ on thin films of PMN-PT grown with the PLD technique is the ultimate goal of the research.

The idea is to compare the results with the results of a recent publication. This publication made the film with molecular beam epitaxy (MBE), and claimed a "Giant Piezoelectricity on Si"[1]. The different parameters used for deposition are in general better controllable with molecular beam epitaxy, so the hypothesis was that the results for a sample made with pulsed laser depositioning would be a bit less than the results claimed in the article.

In the article it is not specified how the $e_{31,f}$ is measured. The value can vary for different measuring methods. If a "giant piezoelectricity" is to be claimed it is probably measured with a method for which the highest results are obtained. There are multiple methods to measure piezoelectric coefficients, for instance active and passive measuring. Therefore it could be possible that a lower, but more realistic value is obtained within this research.

With the deposition in the article it was necessary to use a substrate with a miscut of a few percent to get rid of the pyrochloric phase in the PMN-PT, it is therefore expected that it is very hard to achieve pure perovskite phase on a normal silicon substrate. Furthermore epitaxial growth is desired and achieved in the article. It will be difficult to create the same (001)-orientated epitaxial growth in the relatively small amount of time given. As long as pyrochloric phase and perovskite phase are present at the same time, epitaxial growth will not be obtained. Because the lattice parameters of both phases do not match it is not possible for a crystal to grow in a smooth way. Resulting in a textured film with different crystal orientations.

First goal is to get a pure perovskite phase thin film of PMN-PT. To achieve this the right parameters for growing the material have to be chosen. Next to that the (001) orientation is the desired direction of growth. The parameters for pulsed laser deposition therefore have to be adjusted to get (001)-orientation of the perovskite phase with epitaxial growth. When good results are obtained, (piezo)electric measurements can be done to look at the properties of the PMN-PT and to compare the values to the article in Science.

However, this research is limited by the relative short time period in which this all has to be achieved. It must be possible to get a near pure phase and epitaxial (001)-orientated thin film of PMN-PT. If this succeeds also piezoelectric coefficients can be determined. Expected is that these values will be lower than the values stated in the article. This might be caused by two things. One of them is that the samples will not be fully optimized after this research. And the second reason is that a realistic piezoelectric value is desired. Therefore it might be lower than in the most ‘ideal’ case.

Chapter 2

Theory behind the piezoelectric effect

2.1 Piezoelectricity and polarization

The material PMN-PT is a material belonging to a group of materials with piezoelectric properties. Piezoelectricity is the term for the phenomenon where an applied electric field results in mechanical stress and vice versa. The cause of this property can be found in the symmetry of the crystal. Piezoelectric materials consist of non-centrosymmetric crystals, which means that the center atom is slightly off-center. Therefore there is more than one equilibrium position for the centre atom, to position itself inside the unit cell. Because all of these positions are off-center there is a "build-in" dipole, which causes a polarization in the material without an applied electric field. This is called 'remanent polarization'.

When an electric field is applied the polarization inside the material will change due to this field. The value of the polarization does not only depend upon the strength of the field but also on the history of the polarization. Such a loop is called a hysteresis loop, and an example of such a loop is given in figure 2.1. The loop starts at an applied field of zero [V/m], after which the field is increased. This will result in an increase of polarization. At point 'a' the polarization is saturated. This means that almost all dipoles are poled in the same direction. A decrease in electric field results in a movement from 'a' to 'b' where a few dipoles have flipped state, but almost all other domains are still facing the same direction. When the applied electric field is absent there is still a huge polarization. After a short while this polarization will decrease automatically due to the relaxation period in which the domains will find their equilibrium positions under the new circumstances. At point 'c', the electric field is absent. The polarization here is called the remanent polarization, as mentioned before. When moving on from 'c' to 'd' the applied electric field becomes negative. This results in an even further flipping of dipoles, resulting in a smaller polarization. Eventually it reaches a point in which both dipole directions are equally represented. This point, 'd', is the point where the polarization on macro scale is equal to zero. The corresponding applied field is called the coercive field. Finally when the applied field becomes even more negative the polarization reaches its maximum in the opposite direction. The lower curve eventually moves to ‘a’ in the same way as discussed above for the higher curve.

The switching of most dipoles occurs in the area where the graph is the steepest. The area of this steep line represents the flipping of most domains. The steeper this line, the faster the material reacts. this reaction time would ideally be zero, resulting in a step function for the hysteresis loop. As can be seen this is not the case. Further on, under ‘Results’, hysteresis loops of grown samples will be displayed and discussed.

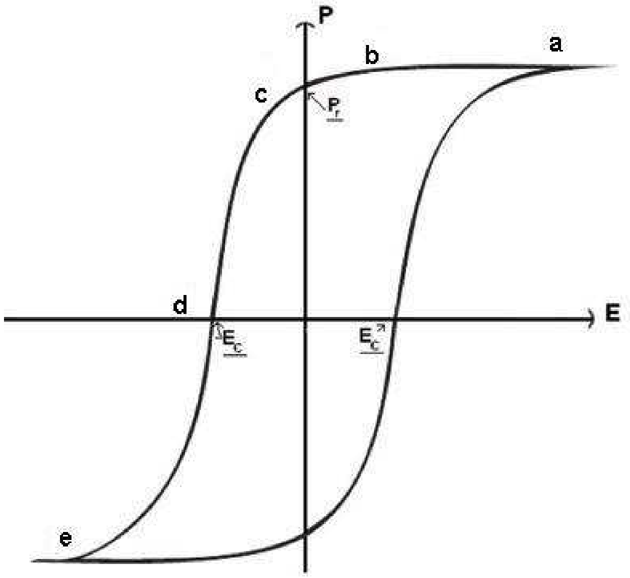

Figure 2.1: Polarization as a function of the applied electric field [3]

The actual piezoelectric effect can be measured when a mechanical stress is applied to the material, while at the same time the induced charge is measured. When this happens the center atoms of each unit cell might ‘flip’ to its new position, thereby changing its dipole moment which in turn induces a charge. The stress can be applied in multiple directions, just like the resulting induced charge can be measured in various directions.

The most common piezoelectric coefficients are called $e_{31,f}$, d_{31} and d_{33}. In these coefficients the first number indicates the direction of the polarization and the second number the direction of the mechanical stress. The subscript ‘f’ means it is measured on a film.

The d-coefficients are determined by measuring the induced charge as a function of the applied force, where the e-coefficient is determined as a function of applied displacement.

2.2 Influence on piezoelectricity

The piezoelectric properties of a material are not conserved under all circumstances. Above a certain temperature, called the Curie temperature, the material loses all its spontaneous polarization and piezoelectric characteristics. This is due to the unit cell changing its shape from non-centrosymmetric to symmetric. Therefore the center atom will not longer be displaced from the center, resulting in loss of dipole moment and therefore also the spontaneous polarization. Near the Curie temperature the piezoelectric properties already decrease. Therefore the operational temperature of a piezo-device has to be well below T_C to get a good efficiency.

Another way of losing the piezoelectric characteristics is by altering the composition of the material. At a certain stoichiometry of the material the crystal structure will change, resulting in a center-symmetric crystal. This phase transition between crystal structures is called the morphotropic phase boundary (MPB). In figure 2.2 both crystal structures are displayed for the material PZT. The left unit cell is cubic and symmetric and does therefore not posses piezoelectric properties. As said before this can be caused by exceeding the Curie temperature or being on the wrong side of the MPB due to the material composition. The unit cell on the right is polarized in the '3' direction, which is illustrated by the arrow on the right pointing upwards. But can also be seen by looking at the 'black atom' which is displaced to above the center of the unit cell.

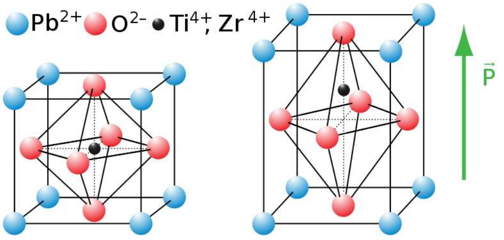

Figure 2.2: Piezoelectric effect in PZT [4].

Even when the material is below T_C and on the good side of the MPB it is still possible the material does not posses piezoelectric properties. This is because there are two possible phases for the material to grow in: the perovskite and the pyrochlore phase.

The piezoelectric properties of a material are much better in the perovskite phase. Therefore, to obtain a high piezoelectric effect, the preferred phase of the film is perovskite and the pyrochloric phase must be avoided. Because the difference between both phases are relatively small it is hard to obtain a pure perovskite phase. The perovskite family is the group of materials which have a molecule formula of ABO_3 [5]. The perovskite structure consists of corner linked BO_6 octahedra. These octahedra form a three-dimensional structure with the

A cation located in the centre of the cavities in the three-dimensional structure. These A cations, which occupy the center atom, have 12 neighbouring oxygen atoms.

Almost similar is the molecule formula of pyrochlore: $A_2B_2O_7$. As can be seen the structure differs from the perovskite phase. In this crystal structure, the octahedra still exist but are angled with respect to the perovskite structure. This tiny difference is the difference between a good piezoelectric material and a useless one [6].

If the film is grown and almost no pyrochlore is present, it can still be that one film performs better than the other. This can be the difference between an epitaxial film and a textured film. Epitaxial growth means that unit cells are all orientated in the same direction over the entire surface and unit cells are piled up in a regular way. If this is not the case, it is called a textured film. Such a film consists of islands on the surface which all have their own orientation. This splits the surface into domains. At the edges of these domains there is some abnormal behaviour, because the transition into another orientation takes place. Therefore this transition boundaries, caused by these different orientations, have a negative effect on the films characteristics [7]. The difference is clearly visible in the SEM pictures 2.3 and 2.4. The column structure in figure 2.4 indicates that there is nice growth in the vertical direction, but there are a lot of different growth directions in the horizontal plane, resulting in these domains. Inside the domain there is epitaxial growth, but not in the total film. This has a negative effect on the properties of the material.

The different layers in figure 2.3 are grown epitaxially. This can be seen from the nice smooth surface and little defects in the layer. Also the PMN-PT layer appears darker on the picture, meaning it has a higher density. Naturally the density must be higher in a film without defects like cracks and holes.

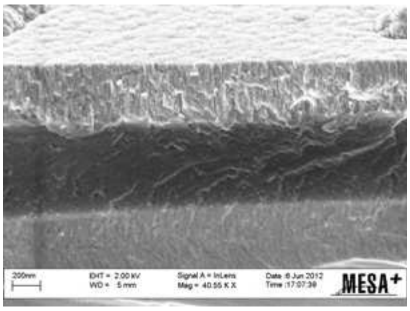

Figure 2.3: SEM picture of epitaxial grown PMN-PT in a sample consisting of LNO/PMN-PT/LNO/STO(001)

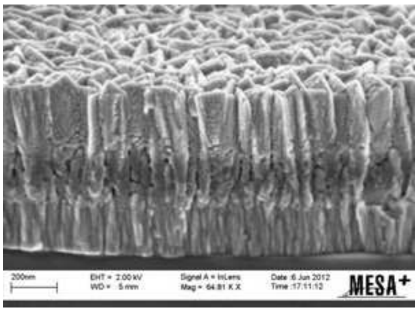

Figure 2.4: SEM picture of textured grown PMN-PT in a sample consisting of LNO/PMN-PT/LNO/Si(001)

2.3 PMN-PT

As already stated in the introduction above, the research is based on the piezoelectric material called PMN-PT, or $Pb(Mg_{1/3}Nb_{2/3})O_3 - PbTiO_3$. As most piezoelectric compounds PMN-PT is mainly based on lead-oxide compounds. In this field of research the most familiar solid is without doubt $Pb(ZrTi))O_3$ (PZT). However PMN-PT is a promising material for which already much higher piezoelectric coefficients have been reached. Nevertheless, this values have never been determined before on a thin film developed with the technique of PLD.

PMN-PT is another type of material than PZT. Where PZT is a ferroelectric material, PMN-PT is a **relaxor** ferroelectric. There are three major differences between these two types of material. Relaxors have not, like a ferroelectric, got a large polarization at zero electric field for the hysteresis loop. This is because all nano-domains are random poled and therefore there is no effective polarization. However, relaxors will be polarized for larger electric fields, but when this field is removed it will lose its polarization directly. The hysteresis loop of a relaxor can be found in figure 2.5. As can be seen a ferroelectric has a much broader area inside the loop.

Next to that, the reaction of a relaxor to the T_C is not a direct transition. The piezoelectric properties of the material will slowly decrease as the temperature rises. Third difference is the difference in temperature and frequency dependence on the dielectric susceptibility. Where ferroelectric materials have a sharp narrow peak near the T_C, relaxor materials have a broad peak [8].

Because PMN-PT consists of two lead-oxide compounds, the ratio between PMN and PT can be varied. The ideal composition is near the Morphotropic Phase Boundary, which can be found around 35% PT in the material [1]. This is therefore the composition used in this research.

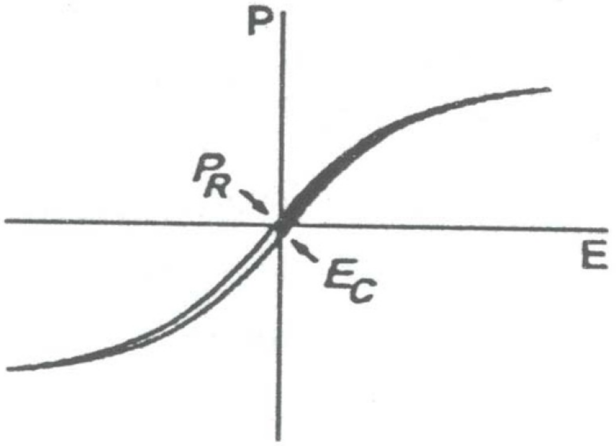

Figure 2.5: Hysteresis loop of PMN-PT, a relaxor material.

What can be seen from the figure directly is the small area within the loop. Therefore the coercive field and the remanent polarization is near zero. Big difference with the hysteresis loop of a ferroelectric material is that no switching moment can be distinguished within for a relaxor.

2.4 Leakage current

Leakage current is the current flowing through the capacitor. This current is an indicator of the amount of pyrochlore phase inside the sample, because the dielectric constant of the pyrochlore phase is lower than the dielectric constant of the perovskite phase [9]. If the dielectric constant is lower, the critical potential between the top and bottom electrode is lower. What means that if the potential becomes higher than a certain value, the capacitor will break down. This effect will occur earlier if the dielectric constant is lower. Pyrochlore will therefore cause the material to breakdown earlier and create a conducting path between both conducting layers. If there is no pyrochloric phase present breakdown will occur at a higher potential because of the higher dielectric constant the perovskite.

Leakage current is a property of the material which has to be made as small as possible to assure a higher efficiency. If the leakage current is large, it's not possible to get a good insight in the quality of the film, because current takes the path of least resistance. If the film has good properties, but there is one conducting path between the top and bottom electrode, it is impossible to measure the properties of the film. Always the higher-conducting path will contribute to the measurements. This is also the reason that bigger leakage currents result in bad piezoelectric properties of the material.

On top of that, leakage current is a direct form of energy loss. Thereby decreasing the efficiency of the electrical circuit when used in integrated circuits. This is no problem in the experimental phase of the research, but becomes a problem when the material is applied in devices.

Leaking current therefore is an important characteristic to determine the quality of the sample. Typical values of good samples are in the range of $\mu A/cm^2$ or smaller.

2.5 Introduction to Pulsed Laser Deposition (PLD)

To apply the PMN-PT thin film, a PMN-PT target is needed to fire at with the laser. The target used in this research is a compressed powder target. This target will be used to deposit a thin layer of PMN-PT on a sample with the technique called pulsed laser deposition, or PLD. This technique is used for making thin films with the help of a laser. The laser beam is focussed on the target material that has to be deposited. The target materials are located inside a low pressure chamber. An overview of the machine used for PLD is shown in figure 2.6. When the beam hits the material it will, due to the extreme temperature rise, increase to millions of degrees in a very short period of time. The material immediately evaporates after which it will be in the plasma phase. Due to the extreme quick temperature rise the different compounds of the material evaporate instantly in such a way that the composition of the material is not altered. After evaporation the plasma plume will then be directed to the substrate caused by the driving force of the material evaporating of the target. When the plasma plume contacts the sample it will cool down real quick again. From theory it is known that it takes a molecule at most a few microseconds to lose most of its energy, settle in and attach to the surface. After this ‘relaxation’ time the molecules are deposited on the surface of the sample. Because the laser works with a certain frequency, smaller than the relaxation time the atoms have time to settle in before a new pulse generates more plasma. This process continues until the grown layer reached the desired thickness.

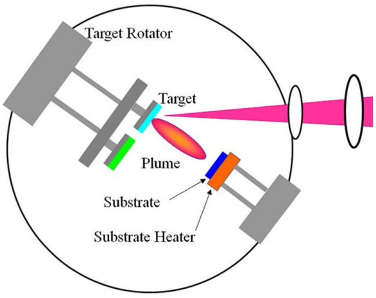

Figure 2.6: A schematic overview of PLD. The laser beam enters the deposition chamber. Here it evaporates the target material into plasma. This plasma plume is then directed to the substrate. The target material can be changed by the rotator. This means the chamber does not need to be opened when changing target material.

The entire process of PLD is really complex, and is not yet entirely understood. Therefore its like a “black box” with a lot of parameters that can be adjusted. The parameters are known, but the exact influence of them are not. Because every material has its own characteristics, the parameters used are different for every material. At the moment a, more or less, “trial and error” approach is used to optimize the process for every material. The PMN-PT used is a new material in the research group and therefore it is not yet known what parameters should be used. This will also have to be optimized during this research, so at the end epitaxial growth of a perovskite PMN-PT film will be possible.

The parameters where deposition depends on are in short described beneath.

First of all the spot size and thereby the shape and quantity of the plasma can be controlled. With a smaller spot size, less material is ablated and also the plasma plume originates from a smaller point. Another energy related parameter is the intensity of the laser. The higher the intensity the more material is ablated, also this ablated material possesses a higher energy. Because of this higher energy, the background pressure must be increased to keep the impact energy of the molecules on the sample the same.

Background pressure is therefore also an important parameter. The background pressure is needed to slow the atoms down before they hit the sample. If the energy of the ablated atoms is too high, the surface of the substrate can be damaged. For non-reactive depositions mostly Argon is used as a background gas.. The background pressure gas can be used to provide a gas to react with the materials that will be deposited. When oxygen-rich materials are deposited oxygen is used to fill vacancies in the material. This means a variation in background pressure also affects the filling of vacancies in the sample.

The temperature of the substrate can be varied to add extra energy to the deposited atoms. In this way the atoms can move a bit around the sample to find the best position. This free-path length is a function of temperature. With higher temperature the atoms will move around more than with a lower temperature.

The frequency of the laser pulses can be varied. With a higher frequency there is more material evaporated in the same amount of time, which results in a faster growth of the layer. On the other hand, the higher the frequency, the less time the molecules have to occupy their best position. Next to that there is not enough time for reactions to fill vacancies in the layer. This can result in a bad quality film.

The distance between the target and the sample is important as well. If the distance between target and sample is too small the plasma plume will hit the sample with an energy which is too high. This energy can then be decreased again by the background pressure. The longer the path length through the chamber the more energy is lost due to interaction with the background gas. Also more background gas is interacting with the plume. This can help with filling vacancies.

When a film is grown with the above parameters optimized there is one last parameter which determines the thickness of the film: the number of pulses. The more pulses fired at the target material, the thicker the film. The right number of pulses depends on the other parameter, because it depends on how much material is deposited per pulse. For example: a film with a thickness of 1 μm can be grown by using a deposition time of 20 minutes at a frequency of 30 Hz, which gives a total of $36 \cdot 10^3$ pulses.

2.6 Direction of growth and lattice constant of crystals

Not every material can just be put on top of another material. There are a few requirements to grow a film. As stated before there are two ways a material can grow on top of another: epitaxial or textured. To obtain epitaxial growth it is very important for the lattice parameters of both materials to match. Else the growth will be chaotic, resulting in a textured film.

Lattice parameters can be matched in two ways. One of them is just to put the unit cells on top of each other. For this to succeed the lattice parameters have to match.

The second option is the growth of the upper layer under an angle of 45°. This way the lattice parameters relate with a factor of $\sqrt{2}$. This way materials with a relative big difference in lattice constant can still be grown on top of each other. When the lattice constant of the substrate does not match with the lattice constant of the film a buffer layer has to be used, which acts as a 'connector', with a lattice constant between the two materials surrounding the buffer material.

Lattice parameters of two different materials never match exactly. There is always a strain on the boundary between the two materials. This stress is called clamping, and affects the characteristics of the film. When a film is made thicker, the clamping effect becomes less relevant because the ratio between the affected area near the boundary and the volume of the entire film is smaller.

2.7 Miller Indices

In the field of crystal structures it is important to identify the orientation of the crystal and its unit cells. With x-ray diffraction it is possible to characterise and identify the crystal orientation using diffraction on the different crystal planes. When this is done it is essential to have a standardized way to name the different orientations so they can be compared to others.

The standardized way to label a crystal orientation is by using Miller indices. These Miller indices are based on three integers written between brackets, for example as (hkl). The integers correspond to a point in space of the reciprocal lattice vectors and with this point, an orientation can be found. The Miller indices in the form of (hkl) are mostly used in this report and also with the characterisation on the XRD machine. The indices written in this manner correspond to a crystal plane [10]. A few examples can be found inside figure 2.7.

The integers are based on a point inside the base of reciprocal lattice vectors. Due to this, it is also possible to see the Miller indices as the inverse of points of intersection in the normal lattice vector space. This makes them quite easy to calculate. It must be taken into account that the inverse is taken, so numbers can also be non integer. The way to solve this is to multiply all 3 numbers by the same factor till all 3 numbers are an integer. The lowest multiplication factor to do so must be taken. This means that $(\frac{1}{1}\frac{1}{3}\frac{1}{\infty})$ becomes (310) in Miller indices.

Also a few variants with other brackets exist, for instance $[hkl]$ or $\{hkl\}$. The brackets are there to indicate on what part of the crystal the numbers act. The numbers between the brackets like $\{100\}$ indicate a set of all crystal planes

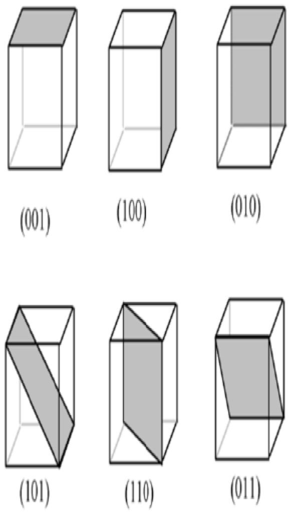

Figure 2.7: A few examples of a crystal plane and its corresponding Miller indices [11].

being orientated equivalent to the direction (100). Each bracket corresponds for another situation.

2.8 Producing a sample with PLD

The samples produced must be suitable for XRD, electric measurements and piezoelectric measurements. In the sample made, this should all be taken into account. This sample requires a top and bottom electrode which are exposed so both electrodes can easily be contacted. With PLD this is achieved by placing a mask over the sample after the bottom conducting layer has been deposited. After depositing the PMN-PT layer another mask is placed to not completely cover the PMN-PT. After depositing the top electrode the sample will look like the sample in figure 2.8.

As can be seen in the figure the grey rectangle at the top is the bottom electrode. The small grey squares and other grey areas are the top and bottom electrodes. Everything else is PMN-PT.

In the figure more than one bending structure is displayed, in fact there are seven bending strips deposited in the same time. Because growing an entire sample takes quite a long time it is ideal that more samples can be grown on a wafer. The wafer used is 25x25 mm and has to be cut into seven separate pieces. Every now and then a sample can accidentally break or be damaged which makes it unusable. When this happens there are still six samples left to measure. Also more samples can be measured to get a more accurate measurement.

Because PMN-PT is a new material within the group, the way to grow a pure perovskite, epitaxial layer is still unknown. The best way to develop such

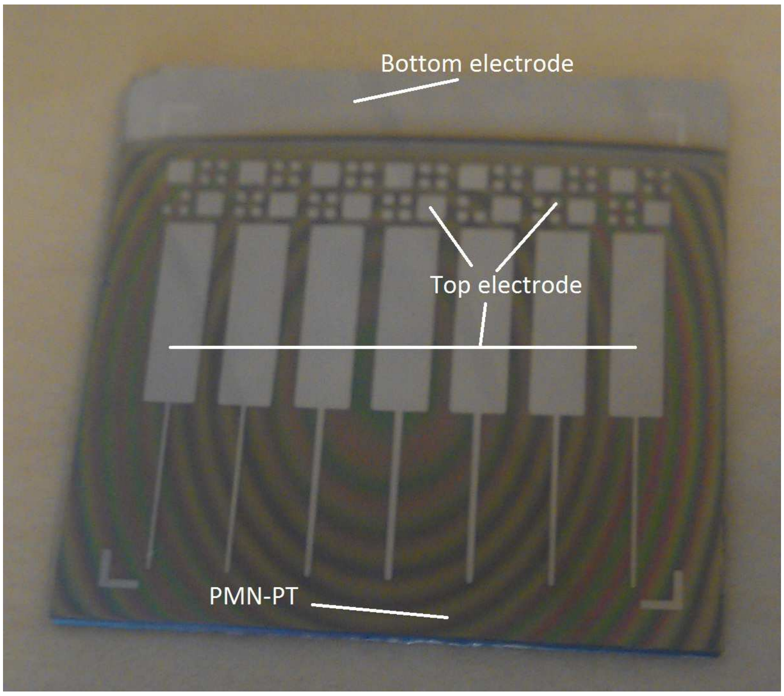

Figure 2.8: Several samples on a wafer which, after cutting, can be used for $e_{31,f}$ measurements.

a sample is to use a step-by-step approach. This is done because the parameters are determined by trial and error. If every layer is in this way optimized, the end result will be a PMN-PT sample with conducting layers grown on silicon.

After every deposition an XRD measurement is done to determine the grown orientations of the material and the phase of the crystals. When the desired result is reached, the next step has to be optimized. All steps used are described below.

2.8.1 STO → PMN-PT

The first step is to start with a very simple sample only consisting of STO as a substrate with the PMN-PT on top of it. The STO used as a substrate is oriented in the 001-direction and epitaxial. Therefore it is an ideal layer for PMN-PT to grow on. Another reason STO is used, is because of the lattice parameter which almost corresponds to that of PMN-PT; 3.9 and 4.0 $\AA$ respectively.

During this step the deposition of the PMN-PT can be optimized by altering the PLD parameters. Eventually STO has to be replaced with another material which is less brittle. Due to the brittleness of STO it can not be bended. Therefore the piezoelectric coefficients $e_{31,f}$ and d_{31} of the PMN-PT can not be measured, while it is possible to determine the d_{33} measurement. When the sample is bend the STO will crack. Furthermore, also the conducting layers are missing. Therefore the next step in developing the sample must be taken.

2.8.2 Si → STO → PMN-PT

The next step is to grow STO and PMN-PT on top of silicon. Eventually silicon must be used as a substrate, because this is a very abundant material and the standard material used in integrated circuit and wafer technologies.

The lattice parameter of silicon with respect to STO is 5.4 and 3.9 $\AA$ respectively. Difference between both lattice parameters is too big to match in a normal way. But when the STO is grown with a 45° angle with respect to the silicon there is a $\sqrt{2}$ relation between both lattice parameters. This will give an effective length of 5.5 $\AA$ for the STO, which nearly matches with 5.4 $\AA$ for silicon. If there is a good match between the lattice parameters, the deposited material will grow in the same orientation as the material it grows on. The PMN-PT will be deposited the same way as under the previous step. Next step will be to add the conducting layers.

2.8.3 Si → STO → SRO → PMN-PT → SRO/Pt

The easiest conducting material to work with is SRO. This material will therefore be used as a start. Other advantages of SRO is that a metal containing oxide shows less loss in material properties due to fatigue of the material in comparison to a metal without oxide like Pt [12, 13]. Next to that, Pt is known for having problems at the Pt/PMN-PT junction being affected by hydrogen [14]. This is not the case for SRO. Another advantage SRO has, is that SRO has nice etching properties. It is possible to etch the PMN-PT on top of the SRO away, hereby exposing the SRO as a bottom contact, without etching the SRO away.

The lattice constant of SRO matches perfectly with the the one of PMN-PT (both 3.9 $\AA$). The top electrode can be any conducting material. It does not matter that much how this top contact is orientated, because it has no effect on the structure of PMN-PT. However the top contact must have good conducting properties and it must be a film with little defects. When this step is optimized still no $e_{31,f}$ or d_{33} measurements can be made, because there is still a layer of STO in the sample. On the other hand, a hysteresis loop can be made to look if the properties look promising. To measure the piezoelectric properties the STO layer has to be replaced or left out of the sample which will be done in the next step.

2.8.4 Si → SRO → PMN-PT → Pt

The last step is to make a sample without the layer of STO. This way the sample is resistant to stress and $e_{31,f}$ measurements can be done in the bender, without breaking the sample. To get good results the growth of SRO on silicon has to be optimized. When this is done the sample is ready for all measurements.

The entire process described above can take quite a long time. In theory there is another method to immediately get better results for the depositioning of PMN-PT and obtain sample where piezoelectric measurements can be performed on. This method is described below. It is a bit of a detour and perhaps not as good as the methods described above. The reason this is done is to get an insight in the properties of the material. If these properties are not as good as expected it might not be profitable to fully develop a method to produce samples without this alternative way.

2.8.5 Si → YSZ → CeO_2 → SRO/LNO → PMN-PT → Pt

Silicon is a material that has a high reactivity with air. Therefore the top layer of silicon will consist of silicon dioxide (SiO_2). Silicon dioxide causes the surface to be amorphous and therefore not a good basis to grow a new layer on. Luckily Yttria-Stabilized Zirconia (YSZ) is a material that absorbs the oxygen from the silicon in an environment with low (oxygen-)pressure and high temperature (820 °C), after which it is possible for YSZ to grow epitaxial on silicon. For the first 30 seconds argon is used, when the YSZ is grown with the PLD system, to create the background pressure to make sure that the YSZ adopts the oxygen from the silicon-oxide. After this initial growth, oxygen is used as a background gas. The lattice constants of both materials are nearly the same, so epitaxial growth is obtained [15].

On top of YSZ a layer of CeO_2 is grown. The lattice parameter of CeO_2 is 5.41 $\mathring{A}$, whereas that of YSZ is between 5.14 and 5.23 $\mathring{A}$ [16]. The lattice parameter of SRO/PMN-PT compared to CeO_2 is a factor of $\sqrt{2}$ smaller. That is why it grows under an 45° angle. The mismatch between SRO/LNO and YSZ is a lot bigger. Therefore CeO_2 acts as a buffer layer between these materials.

On top of the bottom electrode PMN-PT is deposited, followed by a second conducting layer. In the end the entire stack should look like figure 2.8.5.

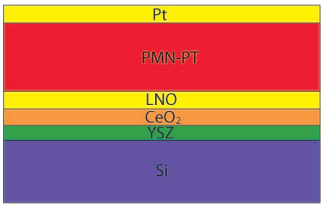

Figure 2.9: How the Si/YSZ/CeO_2/PMN-PT/PT sample is build up

Remark *There are a few remarks on the step-by-step approach. Step two and three (Si/STO/PMN-PT and Si/STO/SRO/PMN-PT) are respectively to use silicon as a substrate and to add a contact layer. Of course it is no problem to inverse these research steps. It is also possible to switch these steps and to first use silicon as a substrate and in after that add a contact layer. Furthermore, in this explanation SRO is used as an electrode layer. For example it is also possible to use LNO or LSMO.*

Chapter 3

Characterisation Methods

When the samples are produced it is key to characterize the properties of the thin film. In theory, PMN-PT has great potential to become the next standard material in piezoelectric devices. The challenge is to make sure these properties are as good in real life as in theory.

First of all the growth of the film will be checked with XRD. Here can be seen if the growth is pure perovksite and its corresponding crystal orientation(s). It can be also seen if the growth is epitaxial. When this is done and the results are promising more tests will be done. One of these tests is to make a hysteresis loop to see how the polarisation responses are of the film. When results are not as expected, a look at the leaking current can be taken to see if this declares the problem. When all results are positive the key measurements can be done. These are of course the $e_{31,f}$, d_{31} and the d_{33} measurement. Beneath an explanation of all techniques is given.

3.1 X-Ray Diffraction (XRD)

The XRD technique is used to determine the parameters of a crystal with the help of x-rays. The x-rays causes the electrons around an atom to vibrate with the same frequency as the incoming wave. Because of destructive interference the waves will cancel out in almost every direction. However in a few directions the interference will be constructive between planes because of the regular organized crystal structure. When a beam is focussed upon the crystal the beam will be refracted in more than one crystal plane. When these crystal planes refract the incident beam, and the difference in path length differs an exact number of wavelengths, they will constructively interfere. This results in equation 3.1, this equation is known as Bragg's law [17].

$$2d \cdot sin(\theta) = n\lambda \tag{3.1}$$

In this equation θ is the angle, λ is the wavelength, d is the distance between the planes of reflection and n is the order and therefore an integer. From this equation 3.1 it is seen that the possible θ values where reflection is possible are determined by the dimensions of the unit cell and their orientation. Not all crystal orientations have the same intensity, even if the presence of the orientations are equal. Therefore the intensity has to be compensated for all peaks so they can be compared with each other. After 'normalising' the intensities a comparison can be made. The way the normalised intensities are determined is by making an XRD spectrum of a powder. In a powder every orientation is present in the same amount. Therefore the reference points are known and the relative intensities can be calculated with the highest peak corresponding to the highest relative intensity.

3.1.1 2θ-scan

After the spectrum of intensity versus θ has been measured there are two ways of using this data. One way is to calculate where peaks of the used materials are expected and to what Miller indices they correspond. This has luckily already been done before for a lot of materials, so the second and easiest way is to just search the database for a diffraction pattern of the materials used and look where the peaks are located. This method is much quicker and will eventually give the same results. Because XRD works with distance between planes it will give the same peaks for different orientations for which distance between planes is the same, like 100, 010 and 001. Furthermore the 200, 020 and 002 peaks are located at double the angle of 100, 010 and 001. If 100 is present, there will always be 'family' peaks present like 200.

3.1.2 ϕ-scan

After this measurement it is still not clear whether the film is epitaxial or textured, because the 2θ peak corresponds to vertical orientations and lattice constants. However from the 2θ spectrum it is not clear if the film is textured or epitaxial. Therefore a second scan has to be made, an in-plane or phi-scan. The first scan made is called an out-of-plane scan. This scan measures the planes parallel to the surface, where the phi-scan measures the planes perpendicular to the surface. When during the phi-scan diffracted x-ray peaks are measured, the film is epitaxial, because the planes face the same direction. If nothing is measured it means the film is textured, because every plane scatters the x-rays to another direction and no constructive interference will occur. If the sample is epitaxial, four peaks can be observed in the spectrum, because of the cubic unit cell. Between these peaks there must be a 90° angle, because when the sample is rotated 90° the beam falls on another side of the cube giving a new intensity peak. Epitaxial films will therefore correspond to peaks measured at 90, 180, 270 and 360° with a ϕ-scan.

3.2 Hysteresis loop

When top and bottom contacts is build in the sample it is also possible to determine the electrical properties. The first characterization will be made with a 'probe station'. This is a device where two contact needles are placed upon the top and bottom conducting layer. Incorporated in this machine there is a microscope to observe the needles approaching the surface of the sample. So it is possible to let the needles contact the surface careful. Which is necessary to avoid damage to the surface by the needles. The sample is made in such a way that both needles can easily contact the top and bottom conducting layers. An example of such a structured sample is given in figure 2.8.

The hysteresis loop is made by varying the electric field and measuring the corresponding polarization of the PMN-PT. This way the polarization as a function of the applied electric field is plotted. From the shape of the loop a few characteristics can be determined. If the hysteresis loop shows two 's'-shaped lines, with a near linear slope in the middle this is a good indication. It indicates that the dipoles flip in an organized way. The steeper the slope, the faster the dipoles flip. Furthermore the remanent polarization and the coercive field can be determined. A good relaxor material gives a P_R and E_C value around zero.

3.3 Measuring the piezoelectric coefficient $e_{31,f}$

To measure the piezoelectric coefficient $e_{31,f}$ it is necessary to apply some form of strain to the sample. This is done by bending the sample.

The machine used works with a four-point bending set-up. The system used is called the 'aixACCT measurement system' [18]. In this system a structured sample is bend on the TF analyser and from this the $e_{31,f}$ can be determined. This bending machine is illustrated in 3.1.

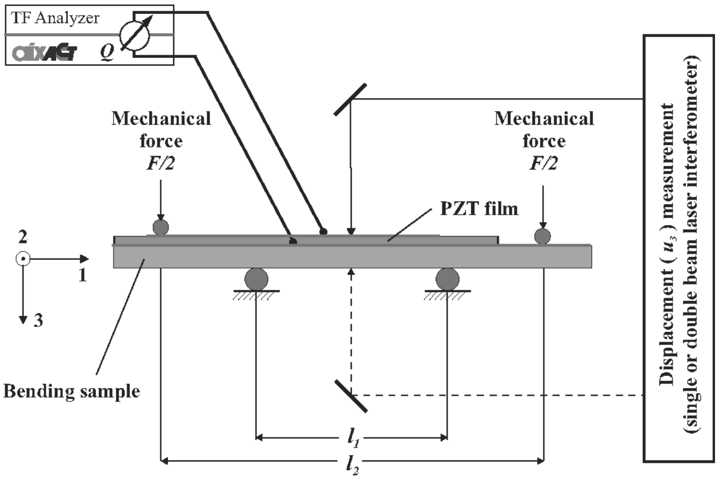

Figure 3.1: The TF-analyser set-up used to measure the piezoelectric effect [2].

As can be seen there are two floating cylindrical benders on the outside and two fixed cylindrical holders in the middle. The cylindrical benders can be brought down to generate a strain in the material. The floating cylindrical bender are made of a conducting material so they can measure the charge induced in the material. This is accomplished by connecting one bender to the top contacting layer and the other to the bottom contacting layer. This is only possible when both contacting layers are exposed on the topside. This is the reason the bottom layer is not completely covered by layers of deposited material as displayed before in figure 2.8. The structure used is made in such a way that it is easy to position the sample correctly inside the bending machine.

The bending of the sample is determined with the help of a laser-interferometer. The laser beam is divided into two beam which take a different path with one beam reflecting off the back of the sample, and then meet again at the sensor creating a interference pattern. If the sample moves, the interference pattern changes and this can be measured with high accuracy. In this way the laser measures the bending of the sample, which is indicated by $u_{3,cant}$. With a simple calculation this can be converted to the applied strain. When the induced charge and the applied strain are known it is possible to calculate the piezoelectric coefficient. The most common way to do this is by making a graph in which the induced charge is plotted as a function of the displacement, an example of such a plot is displayed in figure 3.2. When this is done a linear function is obtained for which the slope is equal to:

$$\frac{Q}{u_{3,cant}} = \frac{4|e_{31,f}|Ah(1-\nu_{Si,f})}{l_1^2} \tag{3.2}$$

Because all other variables are known, the only unknown, $e_{31,f}$, can be determined.

When the TF analyser gives strange results it is recommended to check the contacts and properties in the probe station afterwards. It could easily happen that a contact is cracked due to the applied pressure of the bender. Especially the thin contact line is easily broken.

3.4 Measuring d_{33}

A good way to determine the piezoelectric properties in the z-direction is to measure the displacement as a function of the applied potential, both in the 3-direction. The measured coefficient is therefore called d_{33} and has dimension [m/V] or [C/N], the higher this value the more useful it can be for applications. Both dimensions are actually the same, as is shown:

$$C = \frac{J}{V} \tag{3.3}$$

$$J = N \cdot m; \tag{3.4}$$

$$\frac{C}{N} = \frac{J}{V \cdot N} = \frac{N \cdot m}{V \cdot N} = \frac{m}{V} \tag{3.5}$$

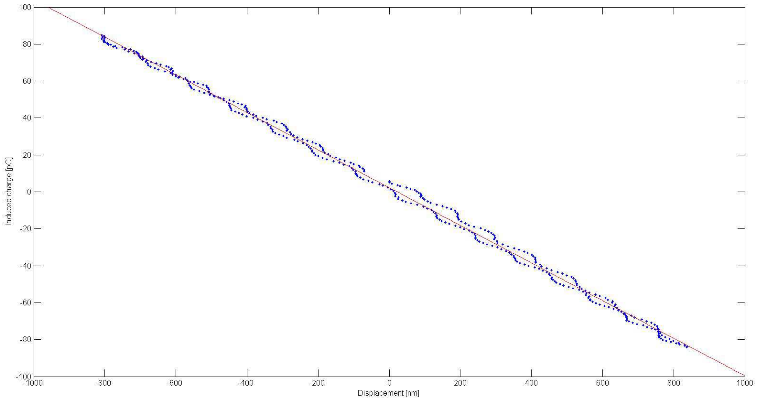

Figure 3.2: Plot of induced charge as a function of displacement for a sample of PZT.

The regime in which the displacement can be found is in the order of picometres [19]. One of the only good ways to detect such a small displacement is with the help of a laser interferometer.

Therefore, just as with the $e_{31,f}$ measurement, a laser interferometer is used. With the help of a laser beam focussed upon the material and the reference beam focussed on another part of the sample where no piezoelectric response takes place. This is done to help eliminate background noise. Because there are a lot of vibrations in the surroundings, this is a nice way to cancel them out. Both laser dots will have the same displacement caused by vibrations from the surrounding. As a result only the actual displacement caused by the field will be measured.

The machine works with a pre-defined raster on which virtual dots are defined by the software used. The laser beam can focus upon these dots to get a contour plot of the height as a function of its position with respect to the probe and the piezoelectric material. This is nice way to see how well the material reacts to the applied voltage.

3.5 Measuring d_{31}

For the determining of the material constant d_{31} it is possible to determine $e_{31,f}$ and obtain d_{31} by calculation, because $e_{31,f}$ and d_{31} are linked via equation 3.6 [2, 20]. In this equation s_{12} can be neglected because the length of the cantilever (around 2 cm) is large compared to the width (a few mm)[20].

$$e_{31,f} = \frac{d_{31}}{s_{11} + s_{12}} \tag{3.6}$$

It is also known that:

$$s_{11} = \frac{1}{Y_p} \tag{3.7}$$

Combining equation 3.6 and equation 3.7 results in the following:

$$e_{31} = d_{31} \cdot Y_p \tag{3.8}$$

So it is possible to calculate d_{31} for a known value of e_{31}, but the Young's modulus must be known. The Young's modulus is a material property and is a measure of the stiffness of an elastic material. The Young's modulus is often well known for the bulk material, but for thin film it is a bit different. Therefore it has to be measured on the sample that is used. This can be done by determining the resonance frequency of the cantilever and using equation 3.9.

When the Young's modulus is not known for the specific sample, it must be determined with the cantilever structure. If the cantilever is made, it is also possible to measure d_{31} directly from this cantilever without measuring e_{31} first. This cantilever structure for d_{31} is necessary, because the displacement has to be measured in the direction parallel to the electrodes. The easiest is to build a cantilever which bends up or down when a negative or positive voltage is applied. By doing this, the displacement can than be measured with an laser interferometer. This technique is usually referred to as the Laser Doppler Vibrometer (LDV) technique.

Usually the dynamic d_{31} is measured. This means an alternating voltage is applied, because the displacement is dependent on the frequency. If this is done, the resonance frequency can be found. From this resonance frequency, the ratio in the Young's modulus can be determined, see equation 3.9. In this equation; L the beam length, t the beam thickness (total), ρ the density, A the Young's modulus ratio of silicon and PMN-PT, B the thickness ratio of silicon and PMN-PT and C is the density ratio of silicon and PMN-PT [20].

All the different constants are known from the dimensions of the cantilever and bulk material of PMN-PT and silicon, except the Young's modulus (Y_p) and the resonance frequency (fr). So if the resonance frequency is measured, the Young's modulus can be obtained.

$$fr = \frac{3.52t}{4\pi L^2} \cdot \sqrt{\frac{Y_p}{3\rho_p}} \left[\frac{A^2B^2 + 2A(2B + 3B^2 + 2B^3) + 1}{(1 + BC)(AB + 1)(1 + B)^2} \right]^{1/2} \tag{3.9}$$

$$\delta = \frac{3L^2}{2t} \cdot \left[\frac{2AB(1 + B^2}{A^2B^4 + 2A(2B + 3B^3) + 1} \right] d_{31}E \tag{3.10}$$

After this the piezoelectric coefficients can be calculated with the use of equation 3.10 (of the Wang and Cross model [21]), in which δ is the deflection at the tip of the cantilever and E is the electric field applied. Now all variables are known except d_{31}. Other models, like the piezoelectric multimorph-model, can be used, but the principle of looking at the resonance frequency is about the same.

There are multiple methods to fabricate the cantilever, of which one is discussed in detail. To process the sample into a cantilever structure it is necessary to first deposit the PMN-PT with a structured top and bottom electrode. After this, the PMN-PT and silicon have to be etched away [22, 14].

Chapter 4

Results

The development of PMN-PT is split up in several steps. All these steps are used to further optimize the parameters used for the deposition. The method used is described before in Chapter 2, under 'Producing a sample with PLD'. All the steps described there can be found as a different section beneath, where one section describes one step.

For every produced sample the deposition parameters for PMN-PT are given in a table. The deposition of the other materials on the sample are not given. These parameters do not influence the growth of PMN-PT as long as their crystal orientations are correct. The parameters used for these other materials are just the standardized parameters used within the research group.

All samples will be characterized with an XRD image. This way can be seen what orientations the crystals of the materials have. All 2θ-scans are represented in figures in the section. The peaks, with their corresponding angles and intensities can be found in 'Appendix'. The global information is all displayed in the figure of the 2θ-scan.

Also a ϕ-scan will be made of the samples. These scans do not give that much information about the sample, they only tell if the growth of the PMN-PT is epitaxial or not. Therefore these scans can be found in 'Appendix'.

When electrodes are present in the sample a P-E loop will be made. These loops can also be found in the section as a figure. At the end of every section a small conclusion will be drawn. Because the parameters chosen for the next sample will depend on the results of the previous.

4.1 STO/PMN-PT

The first sample will be made with PMN-PT directly deposited on STO. The lattice parameter of STO matches quite good with the one of PMN-PT, 3.9 and 4.0 $\AA$. Therefore it is expected that with the right deposition parameters epitaxial growth of a pure perovskite phase must be possible.

The parameters used for the first deposition can be found in table 4.1 and are based upon other articles where PMN-PT is grown with the help of PLD [23, 24, 25, 26].

PLD parameters of PMN-PT grown on STO	
Energy density	2.5 J/cm^2
Spot size	3.3 mm^2
Cooling pressure	1 bar
Target - sample distance	54 mm
Frequency	3 Hz
Temperature	575 $°C$
Background pressure	0.278 mbar
Substrate	STO
Buffer layer	-
Conducting layer	-
Deposition time	30 minutes
Cooling rate	10 ° C/minute

Table 4.1: PLD parameters of PMN-PT grown on STO

Important side note which certainly affected the sample has to be mentioned. Cooling down was accidentally not switched on. Therefore the sample has been at 575°C for about 12 hours overnight. In the morning finally the cooling down process started.

The 2θ-scan made is displayed in figure 4.1. Here the intensity is plotted as a function of the angle. All peaks observed have been put in table 9.1 with their corresponding angle and intensity. Also the materials with its orientation corresponding to the peaks found are displayed in the table.

For the first sample it is a good result. The perovskite phase is already dominant in comparison to the pyrochloric phase in the PMN-PT. Nevertheless, there is some pyrochlore present. This means some adjustments have to be made to the parameters for growing PMN-PT to get better results.

Another reason for the presence of pyrochlore is the prolonged heating time. Lead is volatile at high temperatures and might therefore be evaporated from the sample. The evaporation of lead might have had an influence on the quality of the sample. Therefore another sample with the same parameters will be made. This way the effect of prolonged heating and the 'real' quality of chosen parameters can be examined.

For the second sample the parameters are the same as for the first sample, which can be found in table 4.1. A 2θ-scan can be found in figure 4.2, with the table of corresponding peaks in the 'Appendix' as table 9.1.

At first sight the results look quite similar to the previous sample. The peaks

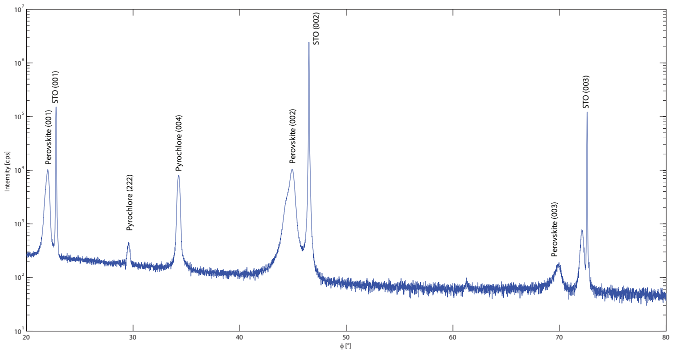

Figure 4.1: 2θ-scan of PMN-PT on an STO substrate.

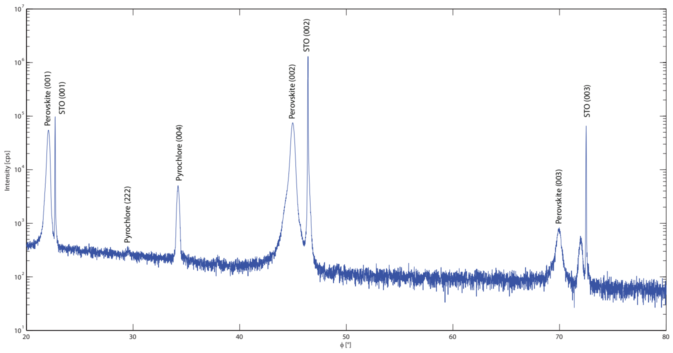

Figure 4.2: 2θ-scan of PMN-PT on STO - second attempt [27]

are present at the same angles. When looked at the intensity of the peaks it can be seen that the pyrochlore peak at 29.2° is much smaller than in the previous sample. This means the sample is an improvement in comparison to the previous sample grown. There is still a large peak of pyrochlore (004) present at 34.1 °. This is the only pyrochloric peak present. Because the 2θ-scan only shows one peak of pyrochlore it is possible to continue to the next step and try to get rid of this peak. This might just be possible because PMN-PT will be grown on another material. The next step will be the adding of a conducting layer between the STO and the PMN-PT.

4.2 STO/LNO/PMN-PT

LNO will be used as the electrode material. LNO is a material with nearly the same lattice constant as PMN-PT, and the same as STO (3.9 $\AA$). With this small mismatch it must be possible to get rid of the large pyrochlore peak which was present in the previous sample. Next to the matching lattice parameters, another reason why LNO is used is because an oxide containing material has better properties in the long term and is more resistant to hydrogen compared to another often used electrode, platinum (Pt) [13, 14]. The PLD parameters used for deposition can be found beneath in table 4.2.

PLD parameters of PMN-PT grown on STO/LNO	
Energy density	2.0 J/cm^2
Spot size	3.5 mm^2
Cooling pressure	1 bar
Target - sample distance	50 mm
Frequency	5 Hz
Temperature	560 $°C$
Background pressure	0.300 mbar
Substrate	Si
Buffer layer	YSZ & CeO_2
Conducting layer	LNO
Deposition time	30 minutes
Cooling rate	6 ° C/minute

Table 4.2: PLD parameters of PMN-PT grown on STO/LNO

Next to a 2θ-scan this time also a ϕ-scan is made. The 2θ-scan be found in figure 4.3 and the ϕ-scan can be found in figure 9.1 in ‘Appendix’. The peak-values found in the 2θ-scan are also placed in ‘Appendix’, in table 9.3.

There is still one pyrochloric peak detected in the spectrum. This means PMN-PT is still not grown in a pure perovskite phase. The only direction of growth for the perovskite phase is the (001)-orientation. The intensity of the pyrochlore peak has decreased. The percentage of pyrochlore present in the film of PMN-PT can not be determined as it is not known what the relative intensities of the pyrochloric peaks are.

There is also a ϕ-scan made of the sample. This scan shows four peaks every 90 °, which means an epitaxial layer has been grown. The reason an epitaxial layer is found while there is no pure perovskite phase detected is because the pyrochloric and the perovskite phase are both orientated in the same way ((001) and (004) respectively). The in-plane scan therefore shows an epitaxial growth.

The results of the grown sample looks good, except for the pyrochlore (004)-peak. Else the film would be pure perovskite and epitaxial in the (001)-direction. Because there are electrodes present in the sample it is possible to determine the electric properties with the probe station. The measurement done is a P-E

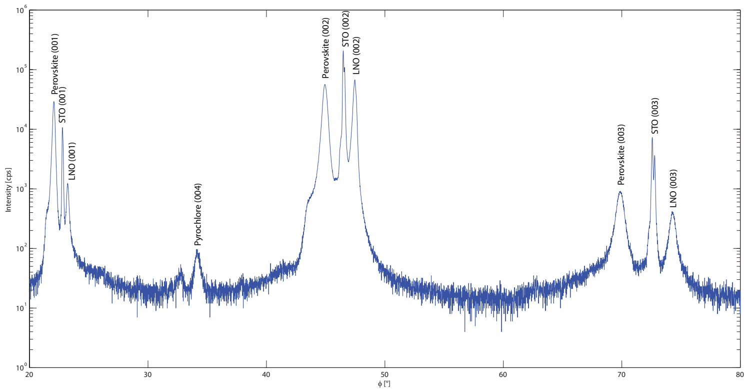

Figure 4.3: 2θ-scan of STO/LNO/PMN-PT [28].

measurement. It could be that the result of this loop will be bad. Reason for this is that the pyrochlore phase causes a larger leaking current. Because some pyrochlore is present this would have a small effect on the hysteresis loop of the PMN-PT. The measured hysteresis loop can be found in figure 4.4.

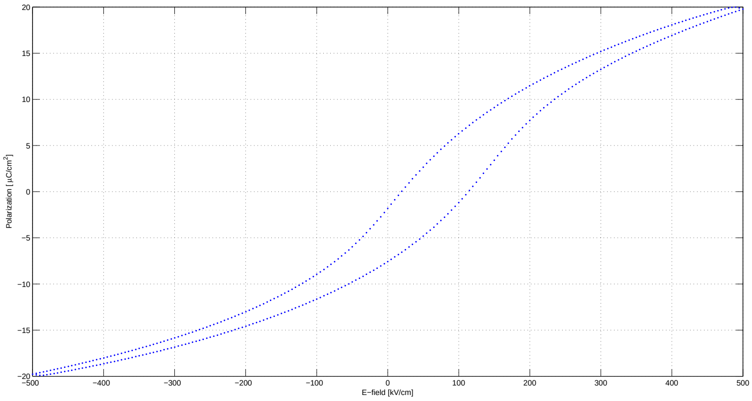

Figure 4.4: Polarization [μC/cm^2] as a function of the applied electric field [kV/cm^2] for the STO/LNO/PMN-PT sample.

The loop has the characteristic shape of PMN-PT. Also the lines are quite close together in the region of the higher electric field, indicating that there is some leakage current but not too much. The displacement of the center of the loop along the electric field axis is due to the polarization measurement which is performed by charge integration, thus requiring an integration constant which is chosen arbitrarily. Therefore the polarization hysteresis loops are usually centred along the polarization axis, as a consequence the loop is shifted along the electric field axis [29, 13]. The maximum polarization found is about 20 μC/cm^2. This can be compared to the result found in the article published in Science where a value of 40 μC/cm^2 has been found. This is for a 1μm thick film, whereas this film grown is approximate 300 nm thick. Therefore this value is really nice. The presence of the pyrochloric peak seems to have little effect on the electric properties of the film, which is a good thing.

It is also possible to do a d_{33} measurement. This measurement will give a first view on the piezoelectric properties of the PMN-PT grown. Result of this measurement is displayed in figure 4.5.

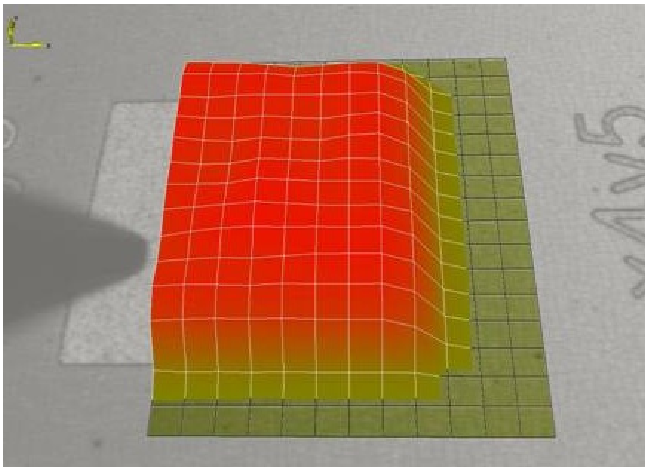

Figure 4.5: Height profile of the STO/LNO/PMN-PT sample during a d_{33} measurement.

The d_{33} coefficient found is equal to 135 pm/V. This value can not be compared to the article in Science while this is not in the article. For PZT the d_{33} coefficient found is already at values higher than 200 pm/V [30]. Therefore the value found for PMN-PT is lower. This is not a fair comparison because PMN-PT is not pure phase and above that is not optimized yet. The results of this sample look good, therefore the next step will be to use silicon as a substrate instead of STO.

4.3 Si/STO/LNO/PMN-PT

This time as a a substrate silicon will be used. On top of this STO is deposited, followed by LNO and PMN-PT. Eventually the STO will have to be removed from the sample because of its brittle character. But this will be done in the next step. The parameters for the deposition are the same as has been used for the previous sample. Results of the deposition can be found in figure 4.6, where a 2θ-scan is displayed. In table 9.3 the corresponding peak-values can be found. To see if the growth of the sample is epitaxial a ϕ-scan is made and can be found in figure 9.2.

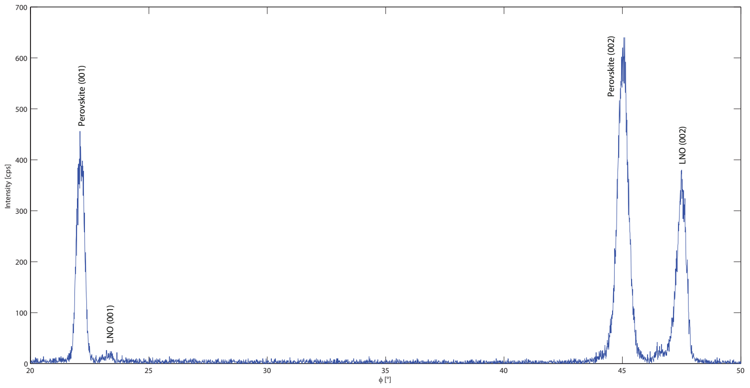

Figure 4.6: 2θ-scan of Si/STO/LNO/PMN-PT [28].

There are only four peaks present in the 2θ-spectrum and correspond to LNO and PMN-PT. The growth of the film is pure perovskite. This is realized without altering the deposition parameters. This is unexpected while the last sample still showed a pyrochloric peak at 34.1°. Consequence of the absence of this peak is that a pure perovskite phase, (001)-orientated film is grown. Expected is that the ϕ-scan therefore shows epitaxial growth. This is also the case as can be seen in figure 9.2.

The contacts on the sample enable the use of the probe station. This hysteresis loop is displayed in figure 4.3. From this loop it can be seen that there is a small leakage current and the switching is as expected for a relaxor material like PMN-PT. It looks like the hysteresis loop of the previous sample, with almost the same hysteresis loop and maximum value. The maximum of this loop is a fraction higher. This could be caused by the absence of a pyrochlore phase, where this was present in the previous sample. The tiny difference is almost negligible.

Just like the previous sample, also of this sample a d_{33} measurement is done. Result is displayed in figure 4.8. The d_{33} value found is 100 pm/V. This value is lower than the value found for the previous sample. Why this value is lower can not be explained from the 2θ-scan and hysteresis loop. The quality of this sample looks better, while it does not posses a pyrochlore phase. This would suggest a higher d_{33} value. Nevertheless the d_{33} coefficient is lower for unknown reasons.

Next step will be to develop a sample without a layer of STO. Because it is not sure whether this sample will be good enough the first time to do piezoelectric measurements on. There is not enough time to make another sample after

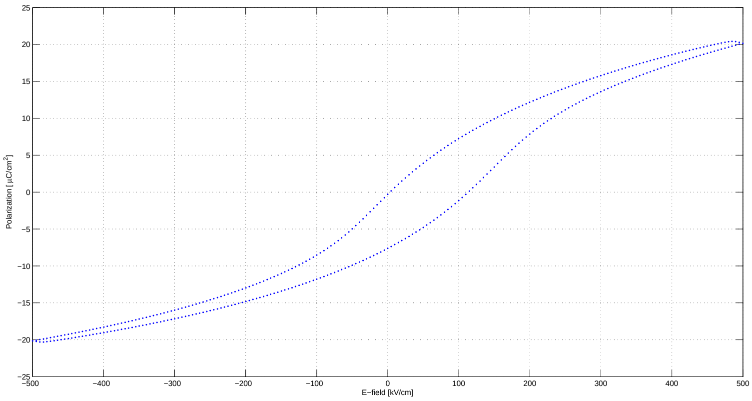

Figure 4.7: The P-E hysteresis loop of the Si/STO/LNO/PMN-PT sample.

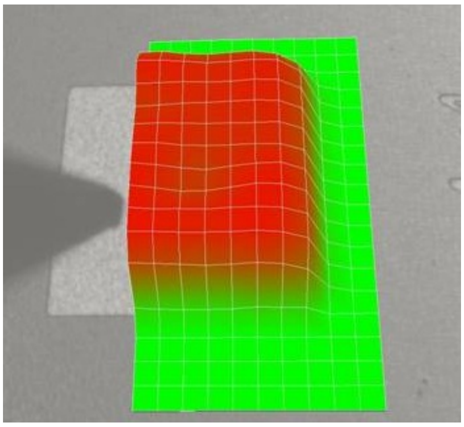

Figure 4.8: Height profile of the Si/STO/LNO/PMN-PT sample during a d_{33} measurement [28].

the next. That is the reason why the choice is made to make a sample with the alternative method. This method is also described under the section 'producing a sample with PLD'.

4.4 Alternative method - Si/YSZ/CeO$_2$/LNO/PMN-PT

Part IV of developing PMN-PT could not be done in the remaining time. Therefore the alternative method for developing a sample is used. This way piezoelectric measurements on the PMN-PT can be done. The deposition parameters can be found in table 4.4. The 2θ-scan can be found in figure 4.9 with the corresponding peaks in table 9.4.

PLD parameters of PMN-PT grown on Si/YSZ/CeO$_2$/LNO	
Energy density	2.0 J/cm^2
Spot size	3.5 mm^2
Cooling pressure	1 bar
Target - sample distance	50 mm
Frequency	5 Hz
Temperature	560 °C
Background pressure	0.300 mbar
Substrate	Si
Buffer layer	YSZ & CeO$_2$
Conducting layer	LNO
Deposition time	30 minutes
Cooling rate	6 ° C/minute

Table 4.3: PLD parameters of PMN-PT grown on Si/YSZ/CeO$_2$/LNO

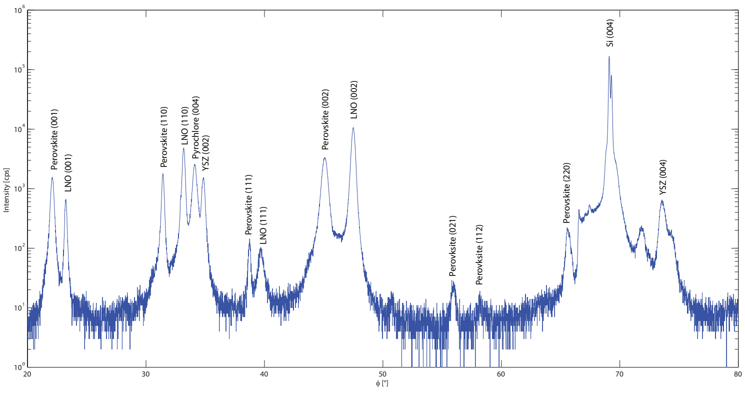

Figure 4.9: 2θ-scan of Si/YSZ/CeO$_2$/LNO/PMN-PT.

The 2θ-scan got a lot of peaks because many materials have been used. This also results in the overlap of some peaks. Which therefore can not be seen in the spectrum. Nevertheless all remaining peaks are labelled with its corresponding material and orientation. As can be seen the pyrochlore is again present in the sample with only the (004)-orientation. Furthermore also the perovskite is not in one orientation any more. Many orientations are found, of which a few are really small. However a few perovskite peaks are quite high, which are the (001), (110) and (111) orientation of the PMN-PT. The normalised intensities of the perovskite orientations are displayed in table 9.4. The 001-orientation of the perovskite PMN-PT is dominant and found to be 73.0% versus 18.2% and 8.8 % for the (110) and (111) respectively.

After the 2θ-scan the top contact is deposited to measure the electric properties. The P-E hysteresis loop can be seen in figure 4.10. The loop are as expected for PMN-PT, but the leakage current is relatively high compared to the Si/STO/LNO/PMN-PT and STO/LNO/PMN-PT samples. This can be seen at both ends of the loops where the loop is wider than for the hysteresis loops seen in the previous samples. The polarization is higher than the other two samples, but the thickness of the two other samples is much smaller. The thickness of the Si/YSZ/CeO_2/LNO/PMN-PT sample is around 800 nm, where the thickness of the other two is approximate 300 nm. The higher leaking current can be declared by two reasons. The film has got a lot more orientations than the previous films and it thicker. More orientations means more distortions in the film. A thicker film results in a higher resistance and thereby to a larger leaking current. Nevertheless, the results look more promising than expected for the spectrum found. The results look good enough to further prepare the sample to eventually measure the $e_{31,f}$ coefficient.

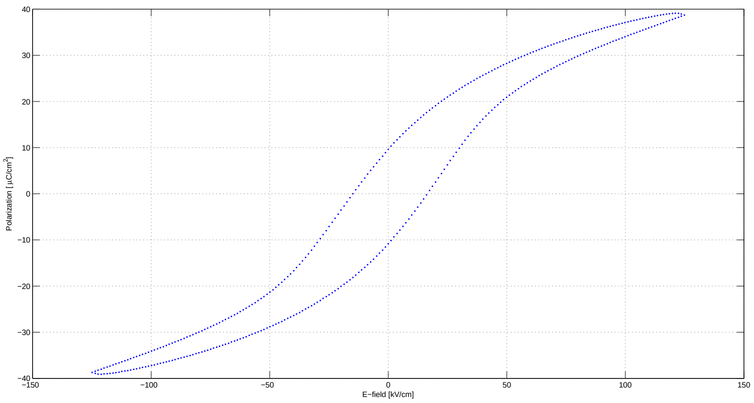

Figure 4.10: P-E measurement for the Si/YSZ/CeO_2/LNO/PMN-PT sample.

Due to problems with the dicing machine it was not possible to further prepare the samples. This will be done on short notice, but not in time to get into this report. When the end goal of the research is to determine a $e_{31,f}$ coefficient of PMN-PT it is unfortunate to not be able to do this. To get an impression on how this would have been done a PZT sample is measured. This can be found in the following section.

4.5 PZT sample to determine $e_{31,f}$

To get an idea on how to determine the piezoelectric coefficient of a material a sample of PZT will be measured. This is done because due to a problem with the dicing machine it was not possible to determine the value for $e_{31,f}$ in time. Therefore a measurement is done on PZT to get an idea on how the measurement is done and how the results can be interpreted. When the PMN-PT sample is diced it can be measured in exactly the same way.

The result of the measured $e_{31,f}$ coefficient can be found beneath in figure 4.11.

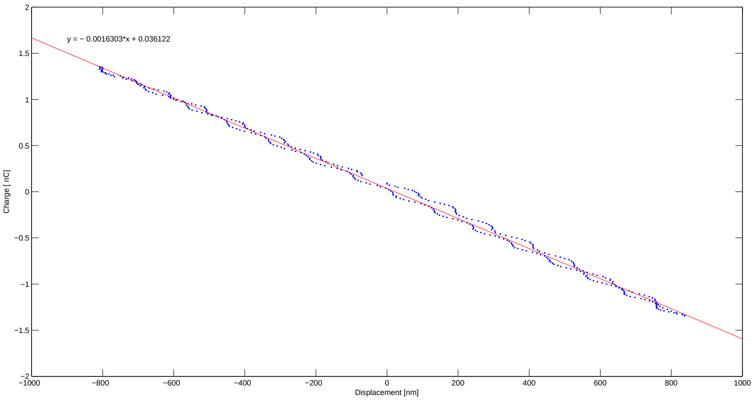

Figure 4.11: $e_{31,f}$ measurement of a PZT sample.

With a slope of -0.001603 nC/nm in the figure it is possible to calculate the $e_{31,f}$ value. This value is put into equation (3.2), and gives a value of 9.8 C/m^2. This is an acceptable value for a sample of PZT. Higher values can already be obtained but this is just an illustration on how to determine $e_{31,f}$. It is expected, as shown in the Science article, that much higher values can be obtained for PMN-PT.

Chapter 5

Discussion & Conclusion

5.1 Discussion

The most samples were not of a pure perovskite phase. This is be there is a (004)-orientation of the pyrochlore phase present. All other pyrochlore orientations are not present in the samples, except for the (222)-orientation in the first two samples. It is not yet known how to get rid of the pyrochlore phase. To get an idea on how to do get rid of the pyrochore phase, more samples will have to be made with different deposition parameters. The temperature used for the samples seems to be good. The pyrochlore phase is promoted by a high temperature, because lead is volatile at these high temperatures. Here 560 °C is not that high for PLD, so this must be no problem. The background pressure of 0.300 mbar seems right when compared to other articles, but might just have to be a little lower to obtain better results. This is the most probable reason for obtaining a pyrochlore phase, when looked at the structure formula: $A_2B_2O_7$ (pyrochlore) versus ABO_3 (perovskite). Here the pyrochlore phase posseses one oxygen molecule more per two A and B molecules. When the background pressure is too high this might just result in a higher oxygen uptake by the film, which might result the pyrochlore phase. The films are rather good, because they only possess two orientations (001) perovskite and (004) pyrochlore. The last sample grown, the sample without STO is the worst sample grown. This sample possesses a lot of orientations in the perovskite phase and also consists partly of the unwanted pyrochlore phase. Most orientations found in the PMN-PT can already be found in the layer underneath PMN-PT. The LNO shows also three orientations, namely: LNO (001), (110) and (111). Therefore the PMN-PT was forced to grow in these directions as well, while it is energetically its favourable position when an underlying atom shows the same orientation. To improve this sample, not only does the parameters for PMN-PT have to be optimized. First of all it is important to obtain epitaxial growth of the LNO. When this succeeds the next step will be to get rid of the pyrochlore (004), like the other samples.

Next to this also the samples have to be prepared to do the e_31, f measurements. Eventually this research focussed on obtaining this coefficient, which was not successful. Progress has been made and the first e_31, f measurement can almost be done. This will give an insight in how good the samples already are, because the quality of the samples has to be improved it would also mean the piezoelectric coefficients will improve.

5.2 Conclusion

At the beginning a number of goals were stated. First goal was to produce an: pure perovskite, (001)-orientated, epitaxial film of PMN-PT. There have been a number of samples produced. These samples are the samples with the following combinatios of materials: STO/PMN-PT, STO/PMN-PT - second attempt, STO/LNO/PMN-PT, Si/STO/LNO/PMN-PT and Si/YSZ/CeO_2/LNO/PMN-PT.

At the moment it was managed with one sample to grow pure perovskite thin films, namely the Si/STO/LNO/PMN-PT sample. All other samples had a pyrochlore phase present in the PMN-PT. In the beginning, for the deposition of PMN-PT directly on STO, there are two pyrochlore orientations, (222) and (004). Later on, for the STO/LNO/PMN-PT and the Si/YSZ/CeO_2/LNO/PMN-PT sample, only one pyrochloric peak matching the (004) orientation is found. In this case, the last sample consisting of Si/YSZ/CeO_2/LNO/PMN-PT showed more orientations in the perovskite phase; not only (001) but also (110) and (111) are present in this sample.

The second goal was to measure the piezoelectric coefficients of the thin films of PMN-PT. Three coefficients would be determined, the $e_{31,f}$, d_{31} and d_{33}. The $e_{31,f}$ coefficient is the most important one as this is the coefficient which has to be compared to the one found in the Science article. The $e_{31,f}$, d_{31} coefficients can only be measured without the presence of STO, because STO will break as it is bended. The d_{33} coefficient is determined for STO/LNO/PMN-PT and Si/STO/LNO/PMN-PT and found to be respectively 135 pm/V and 100 pm/V. These values are lower than the values which can be achieved for PZT at the moment. No articles in which this coefficient is also determined for PMN-PT were found. Therefore the d_{33} coefficient could not be compared to other PMN-PT samples, and is it not known what coefficients are already achieved for PMN-PT.

The $e_{31,f}$, d_{31} coefficients could only be determined for the sample consisting of Si/YSZ/CeO_2/LNO/PMN-PT. As this sample was not fully prepared in time for this report the results could not be published and no $e_{31,f}$, d_{31} coefficients are determined. Therefore there is also no comparison possible with the article in Science.

For all samples containing a conducting layer a P-E measurement has been done. These measurements all gave a good result accourding to the shape of the hysteresis loop. Relaxor behaviour could clearly be seen, corresponding to low P_R, E_C and a small area inside the hysteresis loop. Furthermore the maximum polarization is found to be around 20 μm/cm^2 for the samples STO/LNO/PMN-PT and Si/STO/LNO/PMN-PT with an approximate thickness of 300 nm for the film of PMN-PT. The maximum polarization found for the sample Si/YSZ/CeO_2/LNO/PMN-PT is around 40 μm/cm^2 for an approximate thickness of 800 nm. The article in Science found an polarization of 40 μm/cm^2 for a thickness of 1 μm. The samples in this research would thus have a higher polarization for the same thickness of the film.

Chapter 6

Recommendations

There are a number of things which still have to be done to obtain better results. First of all the deposition parameters for the materials Si, YSZ, CeO_2 and LNO have to be optimized to get rid of multiple orientations in the LNO. This causes the PMN-PT to grow in multiple orientations as well. When LNO can be grown epitaxial in the (001) orientation, PMN-PT will also be able to grow only in the (001) orientation, just like in all other samples. Then there is only one problem left; the presence of the (004) pyrochloric peak. Therefore the deposition parameters of PMN-PT have to be further optimized. Only small changes of a parameter might already give the good result. When optimizing it is also possible to use an other conducting layer, like SRO. It might be that PMN-PT gives better results when its grown on an other electrode material. The Pt used is not an option for this. It is found to promote textured growth for PMN-PT if PMN-PT is grown on top of Pt.

Another thing that needs to be done it to de the piezoelectric coefficients, with the $e_{31,f}$ coefficient as the most important. This has not been done yet. This will give an idea of how good the sample already is in comparison to what is achieved by others, especially in comparison to the article in Science, which stated the have the highest $e_{31,f}$ coefficient at the moment.

The material PMN-PT looks promising, the results in the article are promising and the P-E loops in this research look promising as well. The research is still in the starting phase, and a lot has to be done. The determined d_{33} coefficients are not that high, but also not that important for many devices. Most MEMS need a high $e_{31,f}$ coefficient. Therefore it is very important to get a first value out of the Si/YSZ/CeO_2/LNO/PMN-PT sample already made.

Chapter 7

Acknowledgements

Looking back at 10 weeks of enjoying our stay at the students-room from the Inorganic Materials Science group, there are a lot of new things we have done. Some new insights gained, and new memories made. It was a really nice experience to be a part of such a nice group.

For this we would like to thank Guus Rijnders for exciting us with the initial contact, presenting us a few nice research topics and eventually bringing us into contact with our supervisor.

After this first contact it was the job of our supervisor Matthijn Dekkers to persuaded us to do our Bachelor thesis at the IMS group. This was no problem and the rest is history. After this it was his job to steer us into the right direction and keep track of progress. He did a great job of motivating us and helping us back on track when we lost direction. Thanks for all the help, we would have been unable to do this research without you.

We would like to thank Nirupam for introducing us to the PLD machine and always being helpful when we had any questions.

After we started our research, we found out that there was a new guest inside the group who was also starting research on PMN-PT. It was very helpful to discuss certain PLD settings or XRD-spectra. Therefore we would like to thank Muhammad Boota for helping us by supplying us with some helpful data and some valuable discussions. Our research was done in quite a short time, but he will be busy with PMN-PT for the next 16 months. We wish him good luck with all the obstacles that lie ahead.

Without the help of Minh Nguyen we would not have been able to present the report as it is now in its final state. Thanks for taking the time to build a sample with us. Also thanks for showing us the LDV and presenting us with the needed data.

Last of all we whould like to thank our roommates and the rest of the IMS group to provide a motivating working environment with a nice balance of social interaction at the same time.

Chapter 8

Planning

Schedule	
Week	Activity
1	Orientation. An introduction with our supervisor. Here some literature is given which has to be read to get an idea on the field of research. From this literature more terms are looked up. Which eventually results in the literature research.
2	Literature research and being introduced to some measuring devices like the bending machine, the probe station, the XRD machine.
3	Introduction to PLD and doing the first deposition. This is done with PZT instead of PMN-PT.
4	Doing some measurements on the PZT sample. Search literature for parameters used to deposite PMN-PT.
5	Growing a 25x25 mm PMN-PT sample. Measure (electric) characteristics of the sample.
6	Doing more depositions and measurements, which are processed immediately.
7	Get an introduction to other devices. Doing depositions and measurements. Again processing the data directly.
8	Measuring different PMN-PT samples and make a sample for which the piezoelectric coefficients can be measured.
9	Start writing the report. Maybe do some last measurements.
10	Finish writing the report.
11	Presentation of our research.

Table 8.1: Schedule of the activities done during the bachelor assignment.

Chapter 9

Appendix

Here all ϕ-scans and tables with the 2θ-peaks are displayed. Every sample has its own section to get a clearer view.

9.1 STO/PMN-PT

2θ spectrum of PMN-PT grown on STO			
Peak position [°]	Material (orientation)	Intensity	Normalised
22.0	PMN-PT perovskite (001)	$1.02 \cdot 10^4$	$4.68 \cdot 10^4$
22.8	STO (001)	$1.51 \cdot 10^5$	$1.26 \cdot 10^6$
29.6	PMN-PT pyrochlore (222)	$4.55 \cdot 10^2$	
34.3	PMN-PT pyrochlore (004)	$8.10 \cdot 10^3$	
44.9	PMN-PT perovskite (002)	$1.05 \cdot 10^4$	$4.12 \cdot 10^4$
46.5	STO (002)	$2.42 \cdot 10^6$	$4.84 \cdot 10^6$
70.0	PMN-PT perovskite (003)	$1.90 \cdot 10^2$	$5.59 \cdot 10^2$
72.1	?	$7.79 \cdot 10^2$	
72.6	STO (003)	$1.22 \cdot 10^5$	$1.22 \cdot 10^7$

Table 9.1: 2θ-scan of PMN-PT grown on STO

2θ spectrum of PMN-PT grown on STO - second attempt			
Peak position [°]	Material (orientation)	Intensity	Normalised
22.1	PMN-PT perovskite (001)	$5.47 \cdot 10^4$	$2.51 \cdot 10^5$
22.7	STO (001)	$9.74 \cdot 10^4$	$8.12 \cdot 10^5$
34.2	PMN-PT pyrochlore (004)	$5.04 \cdot 10^3$	
44.9	PMN-PT perovskite (002)	$7.50 \cdot 10^4$	$2.94 \cdot 10^5$
46.4	STO (002)	$1.30 \cdot 10^4$	$2.60 \cdot 10^4$
70.0	PMN-PT perovskite (003)	$8.30 \cdot 10^2$	$2.44 \cdot 10^3$
72.0	?	$5.67 \cdot 10^2$	
72.5	STO (003)	$6.54 \cdot 10^4$	$6.54 \cdot 10^6$

Table 9.2: 2θ-scan of PMN-PT grown on STO - second attempt

9.2 STO/LNO/PMN-PT

2θ spectrum of STO/LNO/PMN-PT			
Peak position [°]	Material (orientation)	Intensity	Normalised
22.1	PMN-PT perovskite (001)	$2.92 \cdot 10^4$	$1.34 \cdot 10^5$
22.8	STO (001)	$1.07 \cdot 10^4$	$8.92 \cdot 10^4$
23.2	LNO (001)	$1.24 \cdot 10^3$	$1.77 \cdot 10^3$
34.1	PMN-PT pyrochlore (004)	$9.70 \cdot 10^2$	
45.0	PMN-PT perovskite (002)	$5.66 \cdot 10^4$	$2.22 \cdot 10^5$
46.5	STO (002)	$2.07 \cdot 10^5$	$4.14 \cdot 10^5$
47.5	LNO (002)	$6.73 \cdot 10^4$	$7.48 \cdot 10^4$
69.9	PMN-PT perovskite (003)	$9.13 \cdot 10^2$	$2.69 \cdot 10^3$
72.6	STO (003)	$7.30 \cdot 10^3$	$7.30 \cdot 10^5$
74.3	LNO (003)	$4.16 \cdot 10^2$	$1.39 \cdot 10^3$

Table 9.3: 2θ-scan of PMN-PT grown on STO/LNO

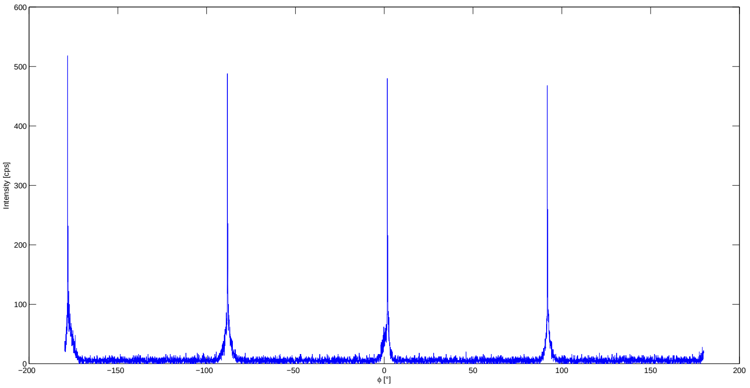

Figure 9.1: ϕ-scan of PMN-PT on STO/LNO [28].

9.3 Si/STO/LNO/PMN-PT

2θ spectrum of Si/STO/LNO/PMN-PT			
Peak position [°]	Material (orientation)	Intensity	Normalised
22.1	PMN-PT perovskite (001)	$4.56 \cdot 10^2$	$2.09 \cdot 10^3$
23.2	LNO (001)	$2.60 \cdot 10^1$	$3.71 \cdot 10^1$
45.1	PMN-PT perovskite (002)	$6.40 \cdot 10^2$	$2.51 \cdot 10^3$
47.5	LNO (002)	$3.80 \cdot 10^2$	$4.22 \cdot 10^2$

Table 9.4: 2θ-scan of PMN-PT grown on Si/STO/LNO.

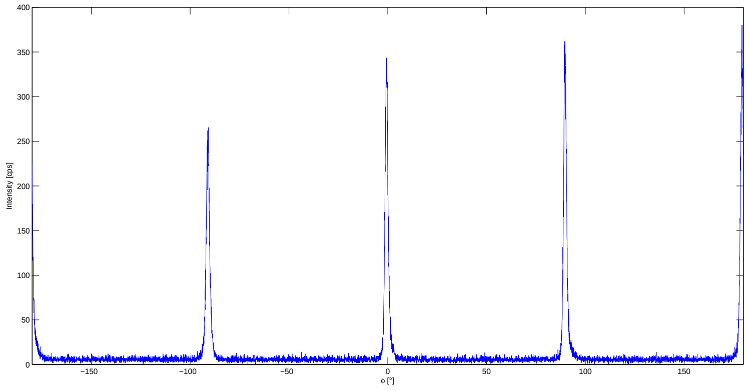

Figure 9.2: 2ϕ-scan of Si/STO/LNO/PMN-PT [28].

9.4 Si/YSZ/CeO_2/LNO/PMN-PT

2θ spectrum of Si/YSZ/CeO_2/PMN-PT			
Peak position [°]	Material (orientation)	Intensity	Normalised
22.1	PMN-PT perovskite (001)	$1.56 \cdot 10^3$	$7.16 \cdot 10^3$ (73.0%)
23.3	LNO (001)	$6.68 \cdot 10^2$	$9.54 \cdot 10^2$
31.4	PMN-PT perovskite (110)	$1.79 \cdot 10^3$	$1.79 \cdot 10^3$ (18.2%)
33.2	LNO (110)	$4.83 \cdot 10^3$	$4.83 \cdot 10^3$
34.1	PMN-PT pyrochlore (004)	$2.59 \cdot 10^3$	
34.9	YSZ (002)	$1.54 \cdot 10^3$	$6.16 \cdot 10^3$
38.7	PMN-PT perovskite (111)	$1.44 \cdot 10^2$	$8.62 \cdot 10^2$ (8.8%)
39.7	LNO (111)	$1.04 \cdot 10^2$	$1.30 \cdot 10^2$
45.1	PMN-PT (002)	$3.33 \cdot 10^3$	$1.31 \cdot 10^3$
47.5	LNO (002)	$1.07 \cdot 10^4$	$1.89 \cdot 10^4$
65.6	PMN-PT perovskite (220)	$2.21 \cdot 10^2$	$1.75 \cdot 10^3$
69.1	Si (004)	$1.69 \cdot 10^5$	$2.11 \cdot 10^4$
71.8	?	$2.41 \cdot 10^2$	
73.6	YSZ (004)	$6.49 \cdot 10^2$	$1.30 \cdot 10^4$

Table 9.5: 2θ-scan of PMN-PT grown on Si/YSZ/CeO_2/LNO

Bibliography

[1] D.M. Kim V.A. Aksyuk R.R. Das S.D. Bu D.A. Felker J. Lettieri V. Vaithyanathan S.S.N. Bharadwaja N. Bassiri-Gharb Y.B. Chen H.P. Sun C.M. Folkman H.W. Jang D.J. Kreft S.K. Streiffer R. Ramesh X.Q. Pan S. Trolier-McKinstry D.G. Schlom M.S. Rzchowski R.H. Blick C.B. Eom S.H. Baek, J. Park. Giant Piezoelectricity on Si for hyperactive MEMS. *Science*, 2011.

[2] Klaus Prume, Paul Muralt, Florian Calame, Thorsten Schmitz-Kempen, and Stephan Tiedke. Piezoelectric Thin Films: Evaluation of Electrical and Electromechanical Characteristics for MEMS Devices. *IEEE transactions on ultrasonics, ferroelectrics, and frequency control*, 207.

[3] University of Cambridge. Ferroelectric materials, 2006. http://www.doitpoms.ac.uk/tlplib/ferroelectrics/.

[4] Author Unknown. Piezoelectricity, 2012. http://en.wikipedia.org/wiki/Piezoelectricity.

[5] Martin Dove. Favourite materials, 2009. http://web.me.com/dove_family/martin/materials.html.

[6] E. R. Vance D. S. Perera, B. D. Begg and M. W. A. Stewart. Application of Crystal Chemistry in the Development of Radioactive Wasteforms. *Advances in Technology of Materials and Materials Processing*, 2004.

[7] University of Geneve. Epitaxial oxide growth on silicon, Year Unknown. http://dpmc.unige.ch/gr_triscone/epitaxialgrowthonsilicon.html.

[8] Matthew Delgado. Phase transitions in relaxor ferroelectrics. 25th of december 2005.

[9] Vinay Chikarmane, Chandra Sudhama, Jiyoung Kim, Jack Lee, and AI Tasch. Effects of post-deposition annealing ambient on the electrical characteristics and phase transformation kinetics of sputtered lead zirconate titanate (65/35) thin film capacitors. *J. Vac. Sci. Technol. A*, 1992.

[10] Micah Baker and Hoble Cohen. An Explanation of Miller Indices Group Activity #1, 2004. http://www.ece.umd.edu/class/enee416.S2004/report1.pdf.

[11] Stefan Kooij. Lecture 1. Lectures of the course “Introduction to Solid State Physics”.

[12] C. S. Ganpule, A. Stanishevsky, S. Aggarwal, J. Melngailis, E. Williams, R. Ramesh, V. Joshi, and Carlos Paz de Araujo. Scaling of ferroelectric and piezoelectric properties in $Pt/SrBi_2Ta_2O_9/Pt$ thin films. *Applied Physics Letters*, 1999.

[13] P.M. te Riele. *Direct Patterning of Oxides by Pulsed Laser Stencil Deposition.* PhD thesis, University of Twente (the Netherlands), 2008.

[14] K. Xiong and J. Robertson. Hydrogen-induced defects and degradation in oxide ferroelectrics. *Applied Physics Letters*, 2004.

[15] T. Hata, S. Nakano, Y. Masuda, K. Sasaki, Y. Haneda, and K. Wasa. Heteroepitaxial growth of YSZ films on Si(100) substrate by using new metallic mode of reactive sputtering. *Elsevier science ltd*, 1998.

[16] A. Kossoy, Y. Feldman, E. Wachtel, K. Gartsman, I. Lubomirsky, J. Fleigc, and J. Maierc. On the origin of the lattice constant anomaly in nanocrystalline ceria. *Physical Chemistry Chemical Physics*, 2006.

[17] Paul J. Schields (State University of New York). Bragg's law and diffraction: How waves reveal the atomic structure of crystals, 2010. http://www.eserc.stonybrook.edu/projectjava/bragg/.

[18] *AixACCT user manual.*

[19] J. Nosek, L. Burianová, M. Sulc, C. Soyer, E. Cattan, and D. Remiens. About the Measurements of the d_{33} Piezoelectric Coefficient of the PZT Film–$Si/SiO_2/Ti/Pt$ Substrates Using an Optical Cryostat. *Ferroelectrics*, 2003.

[20] Romain Herdiera, David Jenkins, Denis Remiens, M. Dupont, and D. Osmont. A silicon cantilever beam structure for the evaluation of d_{31}, d_{33} and e_{31} piezoelectric coefficients of PZT thin films. *IEEE International Symposium On The Applications Of Ferroelectrics.*, 2007.

[21] Qing-Ming Wang and L. Eric Cross. Performance analysis of piezoelectric cantilever bending actuators. *Ferroelectrics*, 1998.

[22] Peihong Wang, Hejun Du, Shengnan Shen, Mingsheng Zhang, and Bo Liu. Preparation and characterization of ZnO microcantilever for nanoactuation. *Nanoscale Research Letters*, 2012.

[23] C. Tantigate and A. Safari. Preparation of $Pb(Mg_{l/3}Nb_{2/3})O_3 - PbTiO_3$ thin films on silicon substrates by pulsed laser deposition. *Microelectronic Engineering*, 1995.

[24] A. Kholkin, C. Tantigate, and A. Safari. Electromechanical properties of PMN-PT thin films prepared by pulsed laser deposition technique. *Integrated Ferroelectrics: An International Journal*, 1998.

[25] C. Tantigate, J. Lee, and A. Safaria. Processing and properties of $Pb(Mg_{l/3}Nb_{2/3})O_3 - PbTiO_3$ thin films by pulsed laser deposition. *Appl. Phys. Lett.*, 1995.

[26] J.P. Maria, W. Hackenberger, and S. Trolier-McKinstry. Phase development and electrical property analysis of pulsed laser deposited $Pb(Mg_{l/3}Nb_{2/3})O_3 - PbTiO_3$ 70/30 epitaxial thin films. *J. Appl. Phys.*, 1998.

[27] Muhammad Boota. Personal communication.

[28] Minh Hguyen. Personal communication.

[29] M. Alexe, C. Harnagea, D. Hesse, and U. G´osele. Polarization imprint and size effects in mesoscopic ferroelectric structures. *Applied physics letters*, 2001.

[30] eFunda database. Lead Zirconate Titanate, 2012. http://www.efunda.com/materials/piezo/material_data/matdata_output.cfm?Material_ID̄PZT-5A.